Scientific Research Publishing

Journal of Power and Energy Engineering, 2024, 12, 1-18
https://www.scirp.org/journal/jpee
ISSN Online: 2327-5901
ISSN Print: 2327-588X

Design and Development of a Parabolic Trough Solar Air Heater for a Greenhouse Dryer

Eric King'ori[1], Isaac N. Simate[2]

[1]Department of Mechanical Engineering, The University of Zambia, Lusaka, Zambia
[2]Department of Agricultural Engineering, The University of Zambia, Lusaka, Zambia
Email: kingorieric49@gmail.com

How to cite this paper: King'ori, E. and Simate, I.N. (2024) Design and Development of a Parabolic Trough Solar Air Heater for a Greenhouse Dryer. *Journal of Power and Energy Engineering*, **12**, 1-18.
https://doi.org/10.4236/jpee.2024.129001

Received: August 8, 2024
Accepted: September 7, 2024
Published: September 10, 2024

Abstract

Design and Development of a Parabolic Trough Solar Air Heater (PTSAH) for a Greenhouse Dryer (GD) was done to improve the dryer's performance. The materials used for the fabrication of the PTSAH included galvanized sheets covered with aluminium foil, an absorber tube made of GI pipe painted matt black to increase heat absorbance at the focal line, mild steel square tubes, shutter plywood, and an axial fan to push air through the absorber tube. Key geometrical parameters used for the design of the PTSAH were a rim angle of 98 degrees, focal length of 0.2608 m, height of 0.3451 m, length of 2 m, and an aperture width of 1.2 m. The PTSAH's total aperture surface area was 2.4 m^2, while its absorber tube surface area was 0.1587 m^2. The PTSAH was experimentally tested to establish its thermal performance. It was found that the ambient air recorded an average value of 31.1˚C and that the air heater could increase the air temperature by 45.6˚C above ambient with a thermal efficiency of 5.3%. It can, therefore, be concluded that the PTSAH can significantly improve the performance of a GD by supplying the GD with air at a higher temperature than ambient.

Keywords

Solar Air Heater, Greenhouse Dryer, Parabolic Trough, Thermal Performance

1. Introduction

Solar dryers are crucial for minimizing postharvest food losses, especially in developing countries where adequate heat facilities for preserving fruits and vegetables are not yet fully established [1]. They have an advantage over other types of dryers since they use solar, which is a renewable and easily accessible source of

energy and are therefore more sustainable and environmentally friendly [2]. Solar dryers can be categorized based on the airflow mode within the dryer as either forced [3] or natural [4] convection. Solar dryers can also be classified based on the way they receive solar radiation as direct, indirect, or mixed-mode [5] [6].

The greenhouse dryer (GD) is of particular interest in this research study. It works on the same principle as the direct type solar dryers, is in forced convection mode and can dry large quantities of agricultural products. To demonstrate the merits of the greenhouse solar dryer, Philip *et al.* [7] provided a thorough experimental analysis of their constructed greenhouse solar dryer's performance and compared them with conventional open sun drying. Fast drying times, better utilization of solar energy, and the creation of higher-quality dried foods were the short-term advantages of the greenhouse solar dryer. The dryer also had notable long-term advantages, such as extended lifespans and quick payback periods. In another instance, the construction of a greenhouse solar dryer and an experimental study of drying fresh Kapenta fish were carried out by Rhoda and Simate [8]. The objective was to assess a suitable thin-layer drying model and compare it to open sun drying. Their findings revealed that the greenhouse dryer significantly reduced drying times compared to open sun drying method. Additionally, the products dried in the greenhouse dryer exhibited higher quality in terms of nutritional content and hygienic conditions when compared to naturally sun-dried samples.

Despite the good drying performance of the greenhouse dryers, they have a shortcoming. The air inside the greenhouses needed for drying is warmed using the greenhouse effect. The operation of the greenhouse dryers requires ambient air to enter them through strategically located air openings. The hot, humid air inside the dryer mixes with the incoming ambient air before being expelled through the dryer's exhaust opening, resulting in a lower drying temperature. A study by King'ori and Simate [9] depicted the limitations of a greenhouse dryer in drying tomatoes. They found that the ambient temperature reached 28.5˚C and 29˚C peaks on the first and second days of drying, averaging at 25.4˚C. In these circumstances, the greenhouse's average temperature rose to 37.2˚C throughout the course of the two days of drying. On the first and second days, the highest temperatures recorded within the greenhouse were 38.4˚C and 45.5˚C, respectively. These temperatures are much lower than the optimum drying temperature of 60˚C determined by Correia *et al.*, [10] as the best to reduce losses and produce the best quality dried tomato. Therefore, to increase the temperature inside the greenhouse to a value of around 60˚C, it is necessary to preheat the ambient air before it enters the greenhouse dryer using specially designed air preheaters.

Air preheaters play a significant role in enhancing the performance and efficiency of a GD. They heat the cool ambient air before it enters the solar dryers to temperatures suitable for drying the different industrial and agricultural products. They can be devices that use solar energy, electricity or fuel to preheat the air. Air preheaters that utilize solar energy are referred to as solar thermal collectors. Solar

thermal collectors can be classified as flat plate solar thermal collectors, with examples [11]-[14] and concentrating/focusing solar thermal collectors with examples [15] [16]. Other devices that preheat air utilize electricity or fossil fuels [17].

Some notable research studies have been conducted to improve the performance of GD. In one of the studies, Simate and Simukonda [11] enhanced the performance of a greenhouse dryer by incorporating a vertical collector to improve the drying process for mangoes. Their research revealed that the drying chamber retained heat more effectively by adding a vertical solar collector, which preheated the air before introducing it into the drying chamber. As a result, the average air temperature within the drying chamber was 14.7˚C higher than the ambient air temperature.

In a similar study, Mehta *et al.*, [12] built a semi-cylindrical GD with an added flat-plate solar collector. They used the dryer to dry fish for performance testing purposes. By creating and solving a mathematical model using the SageMath programming language, they could predict the temperature at the collector outlet. The average collector outlet temperature was determined to be 75˚C. As a result, it took 18 hours to dry the fish compared to 38 hours under open sun drying.

In a further study, ELkhadraoui *et al.*, [14] developed a combination of a tunnel greenhouse dryer and a parabolic trough collector for drying paddy. The system consisted of a single-axis solar tracking system installed on a stainless steel 2.27 m^2 parabolic trough collector. The collector generated hot water, then directed to a crossflow heat exchanger. The heat exchanger had a tunnel GD measuring 2.112 m^2, similar to a flat plate collector. The system aimed to capture solar radiation and redirect it to a receiver positioned at the focal point of the parabolic trough. In addition, a copper heat pipe with an internal diameter of 25.4 mm was installed for water heating. The reported average drying temperature was 57.73˚C.

To conclude with examples of similar studies, Ringeisen *et al.* [16] designed and developed a GD with a solar concentrator. The researchers used Roma tomatoes to test the improved GD's operation. Solar radiation struck the curved concentrated solar collector and was reflected to the tomatoes being dried inside the GD. This implied that there was point heating inside the dryer. It is reported that using the solar concentrator resulted in a higher average temperature inside the GD. As a result, the average drying time was reduced by 21 percent.

A literature review on solar thermal collectors as air preheaters indicates that flat plate solar thermal collectors are predominantly used to improve the GD compared to focusing/concentrating solar thermal collectors. Therefore, concentrating (focusing) solar thermal collectors, specifically the parabolic trough solar collectors, are studied in this research work. Parabolic trough solar collectors have the merit of achieving medium temperatures (100˚C - 400˚C) [18] when heat losses are not taken into account.

This research study aimed to design and fabricate a parabolic trough solar air preheater for a GD and test its thermal performance. The new knowledge on improving the GD performance developed in this study is envisioned to benefit the food processing industry in mitigating post-harvest losses of agricultural products

like tomatoes.

2. Methodology

2.1. Principle Operation of the Parabolic Tough Solar Air Heater (PTSAH)

The PTSAH utilizes solar energy to heat the ambient air. When the sun's rays hit the interior of the aluminium foil-covered parabolic trough collector, they are reflected to the focal line where the receiver tube is located. The receiver tube is painted matt black to enhance solar radiation absorption and is designed to absorb concentrated solar energy. An axial fan pushes ambient air through the heated receiver tube, transferring heat from the hot receiver tube to the ambient air passing through it. Therefore, the system generates hot air at the absorber tube outlet, which can easily be directed to a greenhouse solar dryer to speed up the drying of various agricultural and industrial products.

2.2. Parabolic Tough Solar Air Heater (PTSAH) Design

An existing GD was studied to establish the ideal PTSAH size to be constructed. A literature review on tomatoes that were to be dried was done. It was established from Ringeisen *et al.*, [16], Benedict *et al.*, [19] and Patil and Gawande [20] that the initial moisture content of tomatoes ranged from 90% to 96%, and the final safe moisture content ranged from 10% to 18%. Design calculations were formulated using two drying tables inside the GD, each with a holding capacity of approximately 15kg and initial and final moisture content on a wet basis as 94% and 10%, respectively.

a) PTSAH Area Determination

This section systematically describes how to use equations to determine the size of the PTSAH aperture used to preheat air for drying in the GD.

Step 1: Mass of the water (M_w) to be removed.

The calculation of the mass of water (M_w) to be removed or evaporated from the fresh tomatoes was derived using Equation (1) [21]:

$$M_w = \frac{m_p\left(m_i - m_f\right)}{100 - m_f} \tag{1}$$

M_w is the mass of water to be removed from the fresh tomatoes, m_p is the initial mass of the tomatoes to be dried, m_i is the initial moisture content of fresh tomatoes, % wet basis, m_f is the final moisture content of dried tomatoes, % wet basis.

Step 2: Enthalpy required, h

Equation (2) was used to evaluate the enthalpy (h) of air [19]:

$$h = 1006.9T + w\left(2512131 + 1552.4T\right) \tag{2}$$

where T is the temperature of drying air in ˚C, and w is the humidity ratio of water vapour per kilogram of dry air. Using the psychrometric chart, the initial enthalpy was evaluated at ambient conditions. The final enthalpy was also evaluated using the psychrometric chart at the optimum drying temperature.

Step 3: Drying Rate, d_r

To determine the average drying rate (d_r) of tomatoes, Equation (3) was used:

$$d_r = \frac{m_w}{t_d} \tag{3}$$

where m_w = the mass of moisture evaporated from the tomatoes and t_d = the reasonable estimated time of drying in hours.

Step 4: Mass flow rate, m_a

Equation (4) was used to calculate the required mass flow rate, m_a of air for drying:

$$m_a = \frac{d_r}{w_f - w_i} \tag{4}$$

The initial and final humidity ratios are w_i (kg H_2O/kg dry air) and w_f (kg H_2O/kg dry air), respectively, and d_r is the average drying rate.

Step 5: Volumetric airflow rate, V_a

The evaluation of volumetric airflow rate V_a in m^3/hr is calculated by Equation (5):

$$V_a = \frac{m_a}{\rho_a} \tag{5}$$

where m_a is the mass flow rate of drying air and ρ_a is the density of air.

Step 6: Total useful thermal energy, E

The equation used to calculate the thermal energy of the drying air that is useful, E in Joules, required to evaporate water from fresh tomatoes is Equation (6), [22]:

$$E = m_a \left(h_f - h_i\right) t_d \tag{6}$$

where m_a is the air mass flow rate in kg/hr, h_f and h_i are the enthalpy of drying air and ambient air, respectively, in J/kg of dry air, and t_d is the estimated drying time in hours.

Step 7: Collector area, A_a

The total area required for the PTSAH under solar radiation was calculated from Equation (7) [23]:

$$E = A_a \cdot I \cdot n_{PTSAH} \tag{7}$$

where E is the total useful thermal energy, in Joules, A_a is the PTSAH aperture area in m^2, I is the total incident radiation on the PTSAH surface, and η_{PTSAH} is the PTSAH aluminium foil reflectance efficiency.

b) PTSAH Geometrical Parameters

The parabola's Equation (8) below, described the geometry of the solar parabolic trough, which was used in the fabrication process [24] [25].

$$y = \frac{x^2}{4f} \tag{8}$$

The length (L) multiplied by the width (W_a) resulted in the total collector aperture area (A_a) as follows:

$$A_a = W_a \cdot L \tag{9}$$

After rearranging Equation (9) to determine the aperture area and assuming an aperture width of 1.2 m, the length of the PTSAH was calculated as follows:

$$L = \frac{A_a}{W_a}$$

The calculation of the rim angle (φ_r) utilized the aperture width (W_a) and focal length (f), as shown in Equation (10) below [26]:

$$\varphi_r = \tan^{-1}\left[\frac{8\frac{f}{w}}{16\left(\frac{f}{w}\right)^2 - 1}\right] \tag{10}$$

The focal length, the radius, and the height/depth of the parabola were calculated using Equations (11), (12), and (13) [27] respectively:

$$f = \frac{W_a}{4\tan\left(\frac{\varphi}{2}\right)} \tag{11}$$

$$r = \frac{2f}{1+\cos(\varphi)} \tag{12}$$

The depth or height h parabolic of the parabolic trough collector was given by;

$$h = \frac{W_a^2}{16f} \tag{13}$$

In addition, the focal length of the PTSAH was defined and verified mathematically as follows [26].

$$f = \frac{Y_s^2}{4h} \tag{14}$$

where: f = the focal length of the parabolic trough solar collector, Y_s = the half-length of the collector aperture, h = the height/depth of the PTSAH, φ = the rim angle.

Parabola arc length was calculated using Equation (15) [28]:

$$S = 2f\left\{\sec\left(\frac{\varphi}{2}\right)\tan\left(\frac{\varphi}{2}\right) + \ln\left[\sec\left(\frac{\varphi}{2}\right) + \tan\left(\frac{\varphi}{2}\right)\right]\right\} \tag{15}$$

The equation for the absorber area (A_{ro}), which is the outer area of the tube, is given as follows [29]:

$$A_{ro} = \pi \cdot D_{ro} \cdot L \tag{16}$$

The ratio of the collector aperture area (A_a) to the absorber area (A_{ro}) gives the geometrical concentration ratio (CR) [29]:

$$CR = \frac{A_a}{A_{ro}} \tag{17}$$

2.3. Fabrication of the PTSAH

After designing the parabolic trough solar air heater, the obtained parameters were used in 3D modeling using SolidWorks. The PTSAH was essentially made up of the following major components: solar parabolic trough concentrator, receiver/absorber tube, axial fan, support structure, and adjustable stands, as shown in Figure 1.

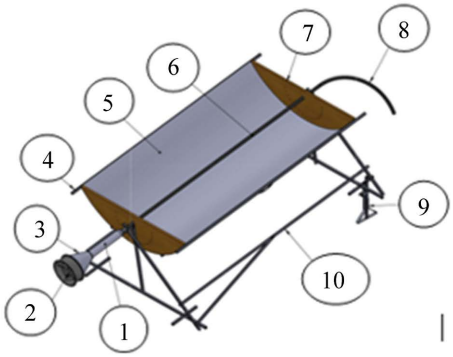

ITEM	DESCRIPTION
1	2'' Sch 5 Pipe
2	Axial Blower
3	Concentric Reducer
4	MS SHS 20×20×2 Trough Reinforcer
5	Aluminium Foil Cover
6	3/4'' GI Sch 5 Pipe
7	Shatter plywood
8	Flexible PVC Pipe
9	Adjustable Stand
10	Fixed Stand

Figure 1. Parabolic trough solar air heater components.

a) Solar Parabolic Trough Concentrator

The solar parabolic trough concentrator was made up of galvanized iron sheets, aluminium foil, shutter plywood, and self-tapping screws.

The solar parabolic trough concentrator had an aperture width of 1.2 m and a height of 0.345 m. A through hole of diameter 0.027 m was drilled at the focal point of each plywood where the receiver tube was to pass. Taking into account the locking mechanism of the PTSAH when manually tracking the sun, 17 through holes of diameter 4.5 mm each were drilled at a radius of 0.211m from the focal point, separated by 10˚ from each other.

Galvanized iron sheets measuring 2 m × 0.9 m each were cut to fit the parabolic curve. Rivets of diameter 0.004 m were used to join the galvanized iron sheets, with the distance between them arbitrarily chosen as 0.1m to maintain uniformity. An aluminium kitchen foil with a reflectance efficiency of 80% was fitted with a Tuff Stuff contact adhesive. Self-tapping screws of diameter 0.004 m by 0.02 m length were used to join the aluminium foil-covered galvanized iron sheets onto the curved surface of the shutter plywood material to take the shape of the parabola. Finally, the solar parabolic trough concentrator was reinforced with four parallel mild steel square tubes of dimensions 2 m × 0.02 m × 0.02 m to prevent possible twisting of the concentrator. Figure 2 shows the fabricated solar parabolic trough.

b) Receiver

The primary goal of the PTSAH was to heat ambient air to a higher temperature. This was achieved by placing a receiver tube concentrically along the focal line of the collector, where the reflected and diffused solar beams were concentrated and converted into heat energy. While different shapes, such as squares,

were possible, a circular section was chosen due to its availability and minimal coverage area to avoid shading on the reflector. A galvanized iron (GI) circular pipe with inner and outer diameters of 0.0216 m and 0.0253 m, respectively, was used. The receiver tube was painted matt black to ensure maximum heat absorption. An axial fan with a reducer was connected to the absorber tube using a two-inch to three-quarter-inch reducer.

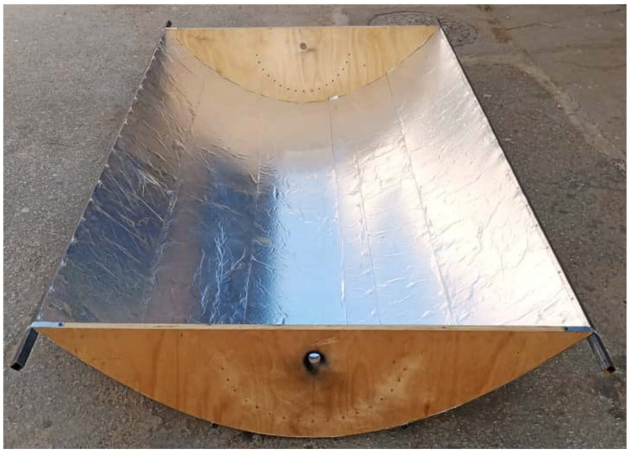

Figure 2. Fabricated solar parabolic trough.

c) PTSAH Support Structure and Adjustable Stands

A rigid supporting structure (Figure 3) was designed and fabricated with rigid flat bars and mild steel square tubes to maintain the collector's stability and accuracy. The joining mechanism of the individual parts employed diameter 4 mm rivets and M6 × 50 mm bolts and nuts. Adjustable stands slanted the PTSAH to the desired slope and inclination angle.

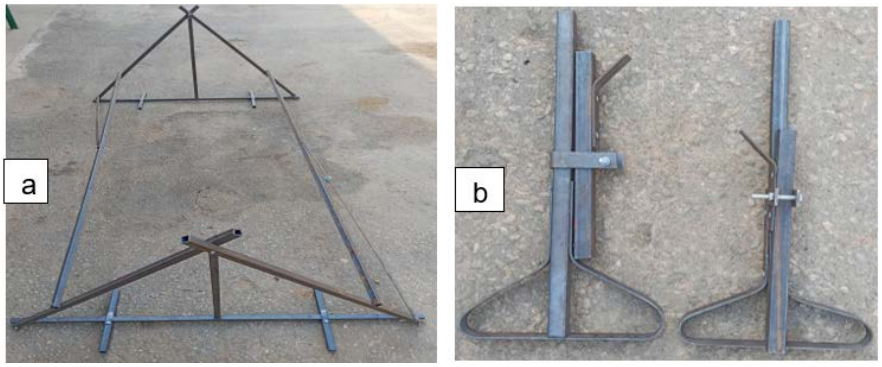

Figure 3. (a) Support structure (b) Adjustable stands.

2.4. Experimental Setup

The experimental setup of the PTSAH consisted of a solar parabolic trough collector, a galvanized iron pipe receiver painted matt black of length 2.15 m, a 220 V powered axial fan connected to one end of the receiver absorber tube, and a support structure with adjustable stands. During the experiment, parameters of

interest were continuously measured, recorded and stored by a multichannel datalogger. These parameters included the temperature of the air at the inlet and the outlet of the absorber tube, the ambient air, the temperature at the receiver's central surface, the amount of solar radiation, and the wind speed. The outdoor testing was conducted in September and October of 2022. The testing system was oriented in the North-South direction at an angle of 15 degrees, equal to the test location's latitude, to capture maximum solar insolation, as shown in Figure 4.

Figure 4. SPTAH experimental setup.

2.5. Instrumentation and Measurement

The temperature was the main parameter of interest in the experimental setup. Pre-calibrated thermocouple temperature sensor probes (Campbell Scientific Inc., model: 108-L accuracy ±0.01˚C) were used to measure the temperature of the ambient air that entered through the axial fan, as well as the receiver tube surface temperature and the temperature of the hot air that exited. For safety reasons, to prevent accidentally touching or holding the hot absorber tube during experiments, a hand-held infrared thermometer (model: UT301A, accuracy of 0.1˚C, range of −18˚C to 350˚C) was used to digitally measure and read the temperatures of the hot absorber tube. The solar radiation and the wind at the test location were also measured using a pyranometer (Kipp & Zonen Delft BV, model: CM11, irradiance range: 0 - 1,400 W/m^2, sensitivity: between 4 and 6 μV/Wm^{-2}) and airflow speedometer (model: KUSAM MECO 909, accuracy of 0.1 m/s, range of 0 - 30 m/s), respectively. Thermocouple temperature sensor probes and the pyranometer were connected to a multichannel data logger (Campbell Scientific Inc., model: CR 1000) that recorded and stored readings at one-minute intervals. The data was retrieved from the datalogger using a laptop via a universal serial bus (USB 2.0) cable for analysis. Figure 5 shows some of the instruments that were used in data collection.

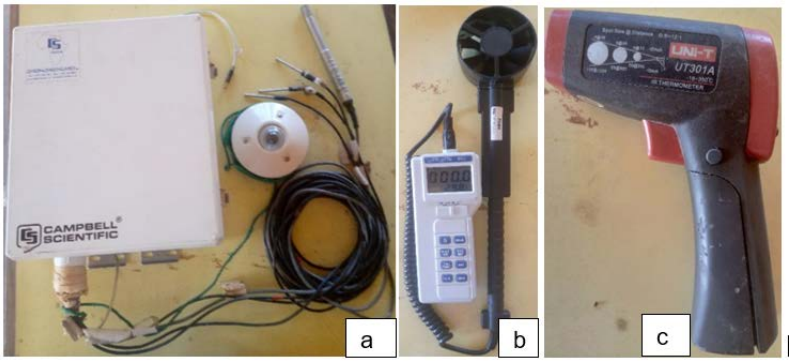

Figure 5. (a) Pyranometer and Thermocouple sensor probes connected to a Multi-channel Datalogger, (b) Airflow speedometer, and (c) Infrared Thermometer.

2.6. Performance Evaluation of the PTSAH

a) Receiver Tube Heat Losses

According to Motwani *et al.* [30], the receiver tube experiences heat loss through convection, conduction and radiation. The energy balance equation explains the heat the transfer fluid dissipates to the tube's outer surface and subsequently to the surrounding environment and is given by Equation (18):

$$Q_T = Q_{conduction} + Q_{convection} + Q_{radiation} \tag{18}$$

where:

Q_T total heat losses by the Heat Transfer Fluid (air) to the surrounding;

$Q_{conduction}$ loss of heat through conduction;

$Q_{convection}$ loss of heat through convection;

$Q_{radiation}$ loss of heat through radiation.

If we ignore heat loss through conduction, we can express the equation above as follows:

$$Q_T = Q_{convection} + Q_{radiation} \tag{19}$$

The equation for calculating convective heat transfer loss ($Q_{convection}$) from the surface of the absorber tube to the surroundings was determined as follows:

$$Q_{convection} = h_c \left(T_s - T_a\right) A_s \tag{20}$$

where:

T_s average absorber tube surface temperature, K;

T_a average ambient temperature, K;

A_s Surface area of the absorber tube given by $\pi d_o L$ (m^2);

h_c the convective heat transfer coefficient of air, which was calculated from Equation (21) [31].

$$h_c = 4d^{-0.42} v_w^{0.5} \tag{21}$$

V_w is the average wind velocity in m/s and d is the outer diameter of the absorber tube in meters.

Radiation heat loss from the surface of the absorber tube to the surroundings

was calculated using Equation (22):

$$Q_{rad} = \sigma \varepsilon_{ab} A\left(T_s^4 - T_a^4\right) \tag{22}$$

where:

σ Stefan Boltzmann constant in W/m^2 K^4;

ε_{ab} 1, the emissivity of the matt black painted GI pipe.

$$A_s = \pi d_o L\left(\mathrm{m}^2\right) \tag{23}$$

b) Thermal Efficiency

The thermal efficiency of a PTSAH (η_{th}) under steady-state conditions is given by Equation (24) [32]:

$$\eta_{th} = \frac{Q_u}{A_{ap} I_D} \tag{24}$$

where:

Q_u is the useful energy transferred to the heat transfer fluid defined as follows;

$$Q_u = \dot{m} C_{p.f} \left(T_{out} - T_{in}\right) \tag{25}$$

$\dot{m}$ air flow rate kg/s;

$C_{p.f}$ specific heat capacity of the air J/KgK;

T_{out} the maximum outlet temperature ˚C;

T_{in} average inlet ambient temperature of ˚C;

A_{ap} collector aperture area of m^2;

I_D average solar radiation on the PTSAH surface W/m^2.

3. Results & Discussions

3.1. Fabricated Solar Parabolic Trough Air Heater

a) Systems Characteristics

The system characteristics of the designed and fabricated PTSAH are shown in Table 1.

Table 1. System characteristics of the PTSAH.

S/No.	Item	Description
1	Rim angle	98˚
2	Focal length	0.261 m
3	Height	0.345 m
4	Aperture width	1.2 m
5	Total length	2 m
6	Total aperture area	2.4 m^2
7	Absorber tube area	0.15899 m^2
8	Absorber pipe inner/outer diameter	0.0216 m/0.0253 m

Continued

9	Concentration ratio	15.1
10	Receiver absorptivity	1
11	Tracking axis	North – South
12	Mirror material	A galvanized sheet covered with aluminium foil
13	Frame material	Mild Steel square tubes and flat plates
14	Heat Transfer Fluid	Air

b) Parabolic Trough Solar Air Heater Assembly

A new PTSAH module was designed and constructed. The individual components, such as the solar parabolic trough collector, receiver absorber tube, axial fan, support structure, and adjustable stands, were fabricated and assembled to make a complete unit. Figure 6 shows the assembled PTSAH.

Figure 6. Different views of the PTSAH assembly.

c) Tracking System

The PTSAH was designed to have an orientation axis of the North-South direction and a rotation direction of the East-West direction to track the sun. The PTSAH was designed to have a manual tracking system. Seventeen (17) through holes with a diameter of 4.5 mm each, 10˚ apart, were drilled onto the shutter plywood at a radius of 0.211 m from the focal point. The locking mechanism utilized a nail as a locking pin, onto the vertical line of the support structure. The parabolic trough was rotated after every 30 minutes. Notably, the trough was freely suspended using the receiver absorber tube. Figure 7 shows the tracking system and locking mechanism of the fabricated PTSAH.

d) Mass of the PTSAH

Due to its modular concept, the complete PTSAH weighed 38.6 kg and could easily be transported to different locations. The design ensured that the system could be scaled in a series or parallel arrangement according to user needs, such as the space available and the quantity of solar energy required to preheat the drying air. Table 2 shows the mass in kilograms of the various components of the PTSAH.

Figure 7. Manual tracking system of the fabricated PTSAH.

Table 2. Mass of the specific components of the parabolic solar air heater (PTSAH).

S/No.	Component	Mass (Kg)
1	PTC housing	20.8
2	Receiver absorber tube	3.2
3	Reducer	3.5
4	Support structure	8.3
5	Two adjustable stands	0.8
6	Axial fan	2.0
	Total	**38.6**

3.2. Temperature Variations

The PTSAH was tested on clear days with the experimental setup described in Figure 4. Figure 8 indicates the variations of temperature analyzed from the data collected on September 13, 2022.

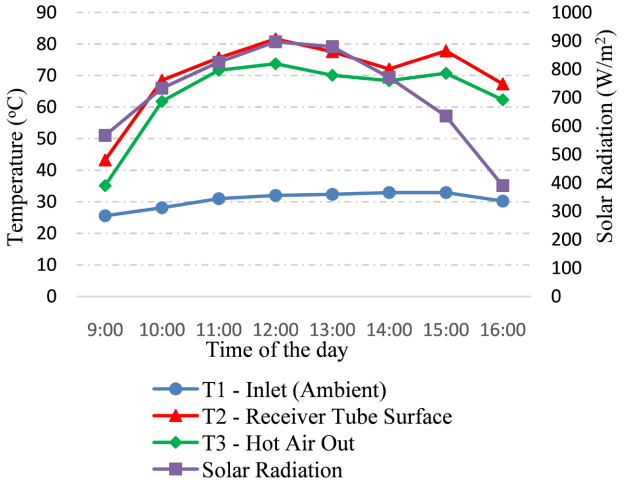

Figure 8. Temperature variation with time of day on the first day of testing the PSTAH.

The experiment's minimum, maximum, and average solar radiation were 346 W/m^2, 906 W/m^2, and 736 W/m^2, respectively. Figure 8 shows that temperatures had a direct relationship with solar radiation; respective temperatures increased as the solar radiation increased and vice versa.

The ambient air recorded had a minimum, maximum and average temperature of 25.5˚C, 34.4˚C and 31.1˚C, respectively. The receiver tube temperatures depended on the timely manual rotation of the PTSAH to track the sun every 30 minutes. A delay in rotating the PTSAH could cause temperatures to decrease, as the data could be read in real time from the laptop connected to the data logger. The minimum temperature of the absorber tube was recorded as 31˚C at 09:00 hrs when the experiment started. At 13:34 hrs, the absorber tube reached a maximum temperature of 85.6˚C. It was observed that the heat transfer fluid (air) forced through the tube absorbed significant heat from the hot absorber tube. The hot air temperature at the exit of the absorber tube ranged between 35.1˚C and 80.1˚C, with the highest temperature being 10˚C lower than that of the receiver absorber tube surface. This temperature difference was due to the heat loss from the bare absorber tube surface to the surroundings. A wind effect of 3.5 m/s during the experiment contributed to significant heat loss from the bare absorber tube surface.

Figure 9 shows various temperature variations of the PTSAH tested on 14th September 2022. The temperatures are consistent with the results of day one, shown in Figure 8.

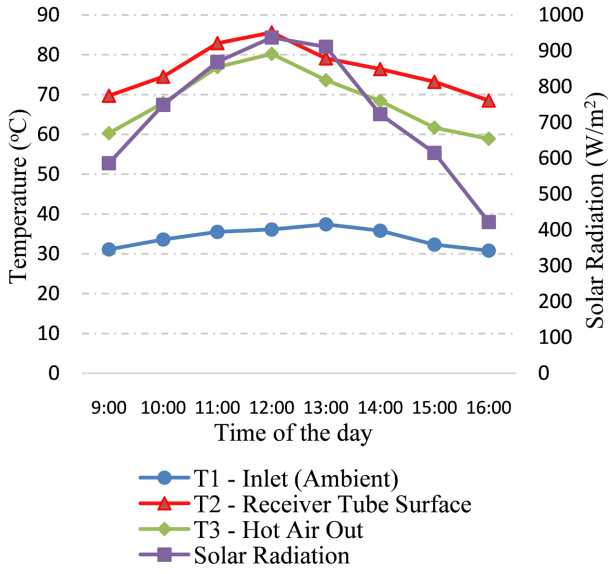

Figure 9. Temperature variation with time of day two during testing of the PTSAH.

The PTSAH raised air temperature by an average of 45.6˚C above the ambient temperature. It was evident that the PTSAH could reliably preheat the ambient air

to considerably high temperatures (45˚C to 60˚C) suitable for drying agricultural products like tomatoes inside a GD.

3.3. Heat Losses

Significant heat was lost from the uninsulated receiver tube to the surroundings, majorly through convection and less through radiation. The total value of heat loss calculated using Equations (20) and (22) was 379.09 W. Eighty-one percent of the heat loss was due to convection heat losses, while the rest was due to radiation heat losses. The high value of convective heat loss was attributed to the wind effect during the performance test. Ambient air that passed over the bare receiver tube carried much heat away. Such a result was expected since the design and fabrication of the SPTAH did not consider the use of transparent glass to cover the parabolic groove where the absorber tube was located. In addition, the absorber tube was not insulated in any way, hence the significant heat losses. Arunkumar and Ramesh [26] reported that heat losses are low in insulated and evacuated absorber tubes; hence, they are more efficient and thus enhance the collector's overall performance.

3.4. Thermal Efficiency

The fabricated PTSAH had a thermal efficiency of 5.3%, as evaluated using Equation (24). It was satisfactory considering the design parameters, particularly the low airflow rate of 0.11346 kg/min. Key factors that determined the thermal efficiency of the fabricated PTSAH were the air flow rate inside the absorber tube and the respective temperatures viz inlet and outlet. In addition, the properties of air as the heat transfer fluid (HTF) used also significantly determined the thermal efficiency of the PTSAH. HTFs with low specific heat capacities, like air, lead to low thermal efficiencies of PTSAH and vice versa. The low value of the specific heat capacity of air contributed to the low thermal efficiency of the PTSAH. Other HTFs like water, oil, salts, and nanofluids have higher specific heat capacities than air, although they are utilized in different applications other than drying.

In a similar study [15], a parabolic trough solar collector air heater was constructed for a GD to dry Paddy rice. The fabricated parabolic trough's thermal efficiency was 8.73%, slightly higher than the current study's. A possible explanation for the slightly higher thermal efficiency value is that water was used as the HTF, which has a higher specific heat capacity than air.

4. Conclusion

A modular solar parabolic trough air preheater was designed, fabricated, and tested to supply hot air to a GD for agricultural and industrial products drying. Local materials and expertise were utilized. Despite the low thermal efficiency and significant heat losses, the PTSAH sufficiently and reliably increased air temperature by 45.6˚C above ambient conditions, making it suitable for industrial and agricultural product drying applications in a GD. The architecture of the assembled

PTSAH was creatively designed with a high level of simplicity to ensure that it can easily be replicated. Further experiments could be done with a bigger diameter absorber receiver tube fitted with fins or metal forms to increase heat transfer to the air.

Acknowledgement

The authors are sincerely thankful and indebted to the Intra-Africa Academic Mobility program for funding this research through a Master of Engineering scholarship at The University of Zambia under the Mobility for Innovative Renewable Energy Technologies (MIRET) program.

Conflicts of Interest

The authors declare no conflicts of interest regarding the publication of this paper.

References

[1] Simate, I.N. and Ahrne, L. (2005) Dehydration of Tropical Fruits. In: Hui, Y.H., Ed., *Food Science and Technology*, CRC Press, 104-1-104-18.

[2] Ndukwu, M.C., Ibeh, M.I., Etim, P., Augustine, C.U., Ekop, I.E., Leonard, A., *et al.* (2022) Assessment of Eco-Thermal Sustainability Potential of a Cluster of Low-Cost Solar Dryer Designs Based on Exergetic Sustainability Indicators and Earned Carbon Credit. *Cleaner Energy Systems*, **3**, Article 100027. https://doi.org/10.1016/j.cles.2022.100027

[3] Salve, S. and Fulambarkar, A.M. (2021) A Solar Dryer for Drying Green Chili in a Forced Convection for Increasing the Moisture Removing Rate. *Materials Today: Proceedings*, **45**, 3170-3176. https://doi.org/10.1016/j.matpr.2020.12.360

[4] Simate, I.N. (2020) Air Flow Model for Mixed-Mode and Indirect-Mode Natural Convection Solar Drying of Maize. *Energy and Environment Research*, **10**, 1-12. https://doi.org/10.5539/eer.v10n2p1

[5] El-Sebaii, A.A. and Shalaby, S.M. (2012) Solar Drying of Agricultural Products: A Review. *Renewable and Sustainable Energy Reviews*, **16**, 37-43. https://doi.org/10.1016/j.rser.2011.07.134

[6] Simate, I.N. (1999) Mixed Mode Solar Drying. Doctoral thesis, University of Newcastle upon Tyne.

[7] Philip, N., Duraipandi, S. and Sreekumar, A. (2022) Techno-Economic Analysis of Greenhouse Solar Dryer for Drying Agricultural Produce. *Renewable Energy*, **199**, 613-627. https://doi.org/10.1016/j.renene.2022.08.148

[8] Rhoda, A.N. and Simate, I.N. (2016) Greenhouse Solar Drying and Thin Layer Drying of Fresh Kapenta (*Stolothrissa tanganicae*). *International Journal of Scientific & Engineering Research*, **7**, 749-756. https://doi.org/10.14299/ijser.2016.05.005

[9] King'ori, E. and Simate, I.N. (2024) Drying Performance and Economic Analysis of a Greenhouse Solar Dryer for Tomatoes. *Journal of Food Sciences*, **5**, 1-15. https://doi.org/10.47941/jfs.1839

[10] Correia, A.F.K., Loro, A.C., Zanatta, S., Spoto, M.H.F. and Vieira, T.M.F.S. (2015) Effect of Temperature, Time, and Material Thickness on the Dehydration Process of Tomato. *International Journal of Food Science*, **2015**, 1-7. https://doi.org/10.1155/2015/970724

[11] Simate, I.N. and Simukonda, K. (2022) Photovoltaic Forced Convection Greenhouse Solar Dryer with an Integrated Vertical Solar Collector for Mango Drying. *European Journal of Applied Sciences*, **10**, 230-244.

[12] Mehta, P., Samaddar, S., Patel, P., Markam, B. and Maiti, S. (2018) Design and Performance Analysis of a Mixed Mode Tent-Type Solar Dryer for Fish-Drying in Coastal Areas. *Solar Energy*, **170**, 671-681. https://doi.org/10.1016/j.solener.2018.05.095

[13] Eltawil, M.A., Azam, M.M. and Alghannam, A.O. (2018) Energy Analysis of Hybrid Solar Tunnel Dryer with PV System and Solar Collector for Drying Mint (MenthaViridis). *Journal of Cleaner Production*, **181**, 352-364. https://doi.org/10.1016/j.jclepro.2018.01.229

[14] ELkhadraoui, A., Kooli, S., Hamdi, I. and Farhat, A. (2015) Experimental Investigation and Economic Evaluation of a New Mixed-Mode Solar Greenhouse Dryer for Drying of Red Pepper and Grape. *Renewable Energy*, **77**, 1-8. https://doi.org/10.1016/j.renene.2014.11.090

[15] Sookramoon, K. (2016) Design of a Solar Tunnel Dryer Combined Heat with a Parabolic Trough for Paddy Drying. *Applied Mechanics and Materials*, **851**, 239-243. https://doi.org/10.4028/www.scientific.net/amm.851.239

[16] Ringeisen, B., Barrett, D.M. and Stroeve, P. (2014) Concentrated Solar Drying of Tomatoes. *Energy for Sustainable Development*, **19**, 47-55. https://doi.org/10.1016/j.esd.2013.11.006

[17] Hamdani,, Rizal, T.A. and Muhammad, Z. (2018) Fabrication and Testing of Hybrid Solar-Biomass Dryer for Drying Fish. *Case Studies in Thermal Engineering*, **12**, 489-496. https://doi.org/10.1016/j.csite.2018.06.008

[18] Zobaa, A.F. and Bansal, R.C. (2011) Handbook of Renewable Energy Technology. World Scientific Publishing. https://doi.org/10.1142/9789814289078

[19] Benedict, E.O., Edward, D. and Oboetswe, M.S. (2019) Development of a Cost-Effective Design of a P-V Ventilated Greenhouse Solar Dryer for Commercial Preservation of Tomatoes in a Rural Setting. *Advances in Technology Innovation*, **4**, 222-233.

[20] Patil, R. and Gawande, R. (2016) Performance of a Forced Convection Solar Tunnel Dryer with and without Thermal Storage for Drying of Tomatoes. *International Journal of Engineering Research in Mechanical and Civil Engineering*, **1**, 111-116.

[21] Fudholi, A., Othman, M.Y., Ruslan, M.H. and Sopian, K. (2013) Drying of Malaysiancapsicum Annuuml. (Red Chili) Dried by Open and Solar Drying. *International Journal of Photoenergy*, **2013**, 1-9. https://doi.org/10.1155/2013/167895

[22] Akoy, E.-A., Ismail, M., Ahmed, E.-F. and Luecke, W. (2015) Design and Construction of a Solar Dryer for Mango Slices. *Mangifera*, **4**, 1-7.

[23] Seveda, M.S. (2012) Design and Development of Walk-In Type Hemicylindrical Solar Tunnel Dryer for Industrial Use. *ISRN Renewable Energy*, **2012**, 1-9. https://doi.org/10.5402/2012/890820

[24] Naranchala, K., Senangkanikorn, N., Krawklom, U. and Choomfon, C. (2020) A Development of Solar Dryer Using Parabolic Mirror Plates. *International Journal of Industrial Electronics and Electrical Engineering*, **8**, 6-10.

[25] Çağlar, A. (2016) Design of a Parabolic Trough Solar Collector Using a Concentrator with High Reflectivity. *World Congress on Mechanical, Chemical, and Material Engineering*, Budapest, 22-23 August 2016, 1-5. https://doi.org/10.11159/htff16.152

[26] Arunkumar, S. and Ramesh, K. (2022) Design and Optimization of Solar Parabolic Trough Collector with Evacuated Absorber by Grey Relational Analysis. *Current*

Science, **122**, 410-418. https://doi.org/10.18520/cs/v122/i4/410-418

[27] Macedo-Valencia, J., Ramírez-Ávila, J., Acosta, R., Jaramillo, O.A. and Aguilar, J.O. (2014) Design, Construction and Evaluation of Parabolic Trough Collector as Demonstrative Prototype. *Energy Procedia*, **57**, 989-998. https://doi.org/10.1016/j.egypro.2014.10.082

[28] Valan Arasu, A. and Sornakumar, T. (2007) Design, Manufacture and Testing of Fiberglass Reinforced Parabola Trough for Parabolic Trough Solar Collectors. *Solar Energy*, **81**, 1273-1279. https://doi.org/10.1016/j.solener.2007.01.005

[29] Bellos, E. and Tzivanidis, C. (2019) Alternative Designs of Parabolic Trough Solar Collectors. *Progress in Energy and Combustion Science*, **71**, 81-117. https://doi.org/10.1016/j.pecs.2018.11.001

[30] Motwani, K., Chotai, N., Patel, J. and Hadiya, R. (2020) Design and Experimental Investigation on Cut Tube Absorber for Solar Parabolic Trough Collector. *Energy Sources, Part A*: *Recovery, Utilization, and Environmental Effects*, **10**, 1-20. https://doi.org/10.1080/15567036.2020.1773964

[31] Yaghoubi, M., Ahmadi, F. and Bandehee, M. (2013) Analysis of Heat Losses of Absorber Tubes of Parabolic through Collector of Shiraz (Iran) Solar Power Plant. *Journal of Clean Energy Technologies*, **1**, 33-37. https://doi.org/10.7763/jocet.2013.v1.8

[32] Duffie, J.A. and Beckman, W.A. (2013) Solar Engineering of Thermal Processes. 4th Edition, Wiley.